

28

29 **Introduction**

30 In light of the control that Earth's changing and variable climate has on the
31 multiple atmospheric and oceanic processes that combine to enhance coastal hazards,
32 there is a need to re-evaluate procedures used to quantify flooding and erosion risk to
33 better protect coastal populations, infrastructure, and ecosystems. Most recent attention
34 has been directed toward potential acceleration in the global mean rise in sea levels (e.g.,
35 Church and White, 2006; Bindoff et al., 2007; Rahmstorf, 2010). This problem has
36 received considerable scientific, public, and political attention, and research has focused
37 not only on predicting the magnitude and time scales associated with sea level rise (SLR)
38 but also on studies quantifying the merits of various mitigation and adaptation strategies
39 (e.g., Nichols and Tol, 2006).

40 A second important phenomenon that has been speculatively linked to (e.g.,
41 Graham and Diaz, 2001; Seymour, 2011), but not formally attributed to (e.g., Knutson et
42 al., 2010), global climate change is increasing storm intensities and the heights of the
43 waves they have generated. An increase in North Atlantic wave heights was first
44 documented by measurements off the southwest coast of England that began in the 1960s
45 (Carter and Draper, 1988; Bacon and Carter, 1991). Wang et al. (2006) and Wang et al.
46 (2009) suggest that the changes in the North Atlantic wave climates, a rate of increase in
47 annual mean significant wave heights (SWH) of about 2.2 cm/year, are associated with
48 the mean position of the storm track shifting northward. Comparable increases have been
49 found in the Northeast Pacific documented by measurements from a series of NOAA
50 buoys along the U.S. and Canadian West Coast (Allan and Komar, 2000, 2006; Mendez

51 et al., 2006, Menendez et al., 2008a; Ruggiero et al., 2010a, Seymour, 2011) and from
52 satellite altimetry (Young et al., 2011). Analyses by climatologists of North Pacific
53 extra-tropical storms have concluded that their intensities (wind velocities and
54 atmospheric pressures) have increased since the late 1940s (Graham and Diaz, 2001;
55 Favre and Gershunov, 2006), implying that the trends of increasing wave heights perhaps
56 began in the mid-20th century, earlier than could be documented with the direct
57 measurements of the waves by buoys.

58 The results of studies relying solely on buoy measurements have, however,
59 recently been called into question after careful analyses of modifications of the wave
60 measurement hardware as well as the analysis procedures since the start of the
61 observations have demonstrated inhomogeneities in the records (Gemmrich et al., 2011).
62 Accounting for these changes trends for the corrected data are smaller than the apparent
63 trends obtained from the uncorrected data. Of interest, the most significant of the non-
64 climatic step changes in the buoy records occurred prior to the mid 1980s. Menendez et
65 al. (2008) analyzed extreme significant wave heights along the Eastern North Pacific
66 using data sets from 26 buoys over the period 1985–2007, not including the more suspect
67 data from earlier in the buoy records. Application of their time-dependent extreme value
68 model to SWHs showed significant positive long-term trends in the extremes between
69 30–45° N near the western coast of the US. Mendez et al. (2010) extended this work by
70 using two time-dependent extreme value models and three different datasets from buoys,
71 satellite missions, and hindcast databases. They conclude that the extreme wave climate
72 in the NE Pacific is increasing in the period 1948-2008 at a rate of about 1 cm/yr (using
73 reanalysis data) and 2-3 cm/yr in the period 1985-2007 (using buoy data).

74 Research on trends in mid-latitude extra-tropical storms in the Eastern North
75 Pacific have confirmed that there has been an increase in storm intensity, but has
76 documented a decrease in storm frequency, possibly since storm tracks have shifted
77 poleward during the latter half of the 20th century. McCabe et al. (2001) showed a
78 statistically significant decrease in the frequency of storms over the years 1959-1997.
79 However, Geng and Sugi (2003) found that the decrease in annual numbers of storms is
80 typically of the weak-medium strength variety, while the stronger storms have actually
81 increased in frequency. Young (2011) recently demonstrated that over the (relatively
82 short) altimetry record both wind speeds and wave heights, particularly the extremes, are
83 increasing along much of the coast of North America. These documented changes in
84 storms are thought to be primarily due to changes in baroclinicity, which in turn has been
85 linked to changes in atmospheric temperature distributions due to increased greenhouse
86 gas emissions. Yin (2005) used the output of 15 coupled general circulation models to
87 relate the poleward shift of storm tracks to forecasted changes in baroclinicity in the 21st
88 century. Though these studies were conclusive that storminess has changed over the last
89 several decades and may continue to change in the future, uncertainties regarding natural
90 variability and model limitations remain.

91 While the exact cause of the increasing wave heights in portions of the Northeast
92 Pacific is still uncertain, the impacts of this phenomenon, particularly in regards to
93 assessments of coastal hazards along the west coast of North America, remain largely
94 uninvestigated. In this paper we quantitatively test the hypothesis that over the historical
95 record (~the last 30 years) increasing wave heights (and periods) have been more
96 important than sea level changes in terms of increasing the vulnerability of the U.S.

97 Pacific Northwest (PNW) coast to erosion and flooding. Predictions are then made, under
98 various ranges of future SLR and rates of wave height increase, regarding the relative
99 roles of SLR and increasing extra-tropical storminess on an increased frequency of flood
100 events and erosion potential over coastal management time scales of decades.

101

102 ***Total Water Level Modeling***

103 The connection between climate change and the potential for increased exposure
104 to coastal hazards is established through application of a total water level (TWL) model
105 (Ruggiero et al., 2001) that involves the summation of the predicted astronomical tides,
106 the non-tidal factors that alter the measured tides from those predicted (most important in
107 the PNW being elevated tides during major El Niños), and the runup levels of the waves
108 on the beach. Estimates of the (hourly) TWL achieved on beaches are taken as

$$109 \quad \quad \quad TWL = \mathbf{MSL} + \eta_A + \eta_{NTR} + R \quad (1)$$

110 where MSL is the local mean sea level (which can be treated as either a constant tidal
111 datum or as a variable with a rate of change), η_A is the astronomical tide, η_{NTR} is the non-
112 tidal residual (NTR) water level, and R is the vertical component of the wave runup
113 which includes both the wave setup (a super elevation of the water level due to wave
114 breaking) and swash oscillations around the wave setup. Here we employ an extreme
115 wave runup statistic, $R_{2\%}$ (e.g., Holman, 1986), the two percent exceedance value of wave
116 runup maxima, since it is the highest swash events in a wave runup distribution that are
117 initially responsible for erosion and overtopping. Simple empirical formulae have been
118 developed for the application of this statistic, for example, Stockdon et al. (2006)
119 combined data from 10 nearshore field experiments and derived an expression for $R_{2\%}$

120 applicable to natural sandy beaches over a wide range of morphodynamic conditions.

121 Their relationship

$$122 \quad R_{2\%} = 1.1 \left(.35 \tan \beta (H_0 L_0)^{1/2} + \frac{[H_0 L_0 (0.563 \tan \beta^2 + 0.004)]^{1/2}}{2} \right) \quad (2)$$

123 relates deep-water wave characteristics and beach morphology to wave runup on the
124 beach; where $\tan\beta$ is the foreshore beach slope, H_0 is the deep-water significant wave
125 height, L_0 is the deep-water wave length, given by Airy (linear) wave theory as $(g/2\pi)T^2$
126 where g is the acceleration of gravity and T is the spectral peak wave period. Being the
127 most widely applicable available formula for wave runup (rmse = 0.38 m), based on the
128 majority of available field data including from the PNW (Ruggiero et al., 2004), the
129 Stockdon et al. (2006) relationship will be used here.

130 The elevation of a particular backshore feature, for example the base of sand
131 dunes or the toe of a sea cliff or shore protection structure, relative to the TWL
132 determines the frequency with which it can be reached by waves, and thus governs its
133 susceptibility to erosion or overtopping (Ruggiero et al., 1996, 2001; Sallenger 2000;).
134 This TWL modeling approach has been demonstrated to be a good predictor of the
135 erosion of weakly lithified coastal bluffs at interannual- to decadal-scale (e.g., Ruggiero
136 et al., 2001, Collins and Sitar, 2008, Hapke and Plant, 2010), dune erosion at annual
137 scale, and event-scale dune response to hurricanes along the U.S. Gulf and Atlantic coasts
138 (e.g., Stockdon et al., 2007).

139 Of primary interest for assessing the impact of climate change on both the historical
140 and future exposure of a coastline to flood and erosion hazards is the time rate of change of the
141 TWL

142
$$\frac{\Delta TWL}{\Delta t} = \frac{\Delta MSL}{\Delta t} + \frac{\Delta \eta_A}{\Delta t} + \frac{\Delta \eta_{NTR}}{\Delta t} + \frac{\Delta R}{\Delta t} \quad (3)$$

143 where $\frac{\Delta MSL}{\partial t} = RSLR = SLR_G + SLR_R + VLM_R$ and RSLR is the local relative sea level rise rate.

144 RSLR can be either positive or negative as it combines the rate of vertical water motions due to
 145 global processes (SLR_G , e.g., increased water temperatures and melting glaciers and ice caps),
 146 regional processes that cause variations from the global mean (SLR_R , e.g., changes to earth's
 147 gravitational field), and vertical land motions (VLM_R , e.g., local tectonics, isostasy, and
 148 compaction). While there is some evidence indicating that the range of astronomical tides may
 149 be evolving (e.g., Flick et al., 2003), of the terms in Eq. 3 both $\frac{\Delta \eta_A}{\Delta t}$ and the VLM_R component
 150 of RSLR can be considered unaffected by a changing climate at the time scales relevant to this
 151 study.

152 The NTR component of the TWL is composed of a complex interplay of processes
 153 often dominated by storm surge (atmospheric pressure effect and wind setup) but also
 154 including effects of local water density variations and coastal trapped waves (e.g., Enfield and
 155 Allan, 1980). Climate-induced changes in any of these processes could lead to measurable
 156 changes in local water levels observed at tide gages. While this meteo-oceanographic 'noise' is
 157 often minimized in tide gage analyses meant to assess regional or global SLR rates, here we are
 158 interested in trends in local TWLs and $\frac{\Delta \eta_{NTR}}{\Delta t}$ is treated as a component of SLR_R and
 159 subsumed within long-term estimates of RSLR. Therefore, the time rate of change of the TWL
 160 achieved on beaches can be simplified to being primarily a function of RSLR as directly
 161 determined from tide gages and the rate of change of offshore wave characteristics (significant
 162 wave height (SWH) and peak period), for particular beach morphology, via their control on the

163 wave runup (Eq. 2). Any trends or variability in these parameters will directly influence the
164 frequency that backshore properties experience erosion or flooding.

165 As in several previous investigations (e.g., Allan and Komar, 2006, Mendez et al.
166 2006, Ruggiero et al., 2010a), the increase in wave characteristics off the PNW is first
167 documented with data from National Data Buoy Center (NDBC) wave buoy #46005,
168 located about 400 km west of the mouth of the Columbia River. This buoy became
169 operational in the mid-1970s and is one of the longest quality wave records in the world.
170 The corresponding hourly $R_{2\%}$ wave runup computations are derived from the buoy data,
171 for representative PNW foreshore beach slopes. Computed RSLR rates are based on the
172 measured tide levels from various National Ocean Service (NOS) tide gage records, and
173 recent investigations have derived updated and improved values for trends in the RSLs
174 for each of the gauges (Komar et al., 2011).

175 Predictions regarding the relative importance of accelerated SLR and increases in
176 storminess to enhanced future coastal vulnerability are made by examining the influence
177 of these factors on a bulk statistic derived from a 10-year TWL time series. This hourly
178 time series, extending from 1 July 1994 to 30 June 2004, has been constructed using the
179 methods developed by Allan and Ruggiero (2010) and Harris (2011). Data gaps in NDBC
180 wave buoy #46005 are filled with NDBC buoys 46089 and 46050 which are landward of
181 the edge of the continental shelf. Hourly estimates of $R_{2\%}$ computed from wave
182 characteristics are simply added to hourly measured water levels from NOS tide gage
183 9435380 in Yaquina Bay, OR to generate hourly estimates of the TWL. The average
184 number of hours per year (impact hours per year, hereinafter IHPY) in which the TWL,
185 for a particular beach slope, reaches or exceeds a particular backshore elevation serves

186 here as a proxy for the probability of beach erosion or backshore flooding (e.g., Ruggiero
187 et al., 2001). The 10-year time period used to compute this proxy includes the major El
188 Niño of 1997/1998 (Komar, 1998; Kaminsky et al., 1998) and the La Niña of 1998/1999
189 (Allan and Komar, 2002) as well as subsequent mild years, and is taken here as
190 ‘representative’ of a typical PNW TWL decade. This ‘gap filling’ approach allows for a
191 10 year time series that is approximately 94% complete.

192

193 **Results**

194 In the following sections the primary components comprising the TWL during the
195 recent historical period, captured by wave buoy and tide gage observations, are first
196 compared and contrasted. Next, the relative influence of possible SLR and increasing
197 storminess on predictions of future risk of coastal flooding and erosion is explored.

198

199 ***Historical changes in TWL***

200 Variations in VLM rates along the PNW coast due to its tectonic setting (e.g.,
201 Burgette et al., 2009) result in along-coast variations in rates of RSLR. Along the
202 southern and northern stretches of the PNW coast, tectonic uplift rates exceed recent rates
203 of regional SLR and land is emergent. By separately analyzing summer-averaged water
204 levels for robust estimates of multi-decadal PNW RSLR, Komar et al. (2011) found that
205 the Crescent City, CA tide gage is experiencing a RSLR rate of approximately -1.1 ± 0.50
206 mm/yr. Along the central to northern Oregon coast sea level is rising relative to the land,
207 for example, the Yaquina Bay, OR tide gage is experiencing approximately 1.33 ± 0.79
208 mm/yr of RSLR (Figure 1, top panel). Along the Oregon/Washington border the Astoria,
209 OR tide gage suggests emergence, while at the Toke Point, WA tide gage, about 50 km

210 north of the Columbia River, sea level is again rising relative to land at a rate of $1.48 \pm$
211 1.05 mm/yr, similar to the rate documented for the Yaquina Bay, OR tide gage.

212 Ruggiero et al. (2010a) found that at NDBC wave buoy #46005 the annual
213 average SWH is increasing at rate of 1.5 ± 1 cm/yr (Figure 1, middle panel). Of more
214 concern in regards to coastal hazards, winter waves observed at this buoy are increasing
215 at a rate of 2.3 ± 1.4 cm/yr. In fact, the rate of increase of the wave climate depends on
216 the exceedance percentile of the SWH cumulative distribution function (CDF) as the
217 bigger waves are getting bigger faster. Annual averaged spectral peak wave periods have
218 been increasing at a rate of approximately 0.015 seconds per year.

219 Of importance, when wave height and period are combined to compute wave runup
220 (Eq. 2), a direct comparison can be made between the sea level and wave induced components
221 of the TWL at multi-decadal scale. Figure 1 (bottom panel) illustrates that the long-term trend
222 in annual mean wave runup, using a representative PNW foreshore beach slope of 0.05
223 (1V:20H), is approximately 3.4 mm/yr. The early part of NDBC wave buoy #46005's record,
224 as called into question by Gemmrich et al., 2011, is not used in this calculation of trends in
225 runup as wave period was not recorded by the buoy until the early 1980s (Figure 1). Therefore,
226 for north-central Oregon beaches with this beach slope (on average), wave induced processes
227 have been over 250% more important than RSLR in producing multi-decadal changes in
228 TWLs. The relative importance of wave induced versus sea level induced impacts on the TWL
229 as a function of foreshore beach slope is illustrated in Figure 2 over a wide range of (average)
230 beach slopes. Only where beach slopes are very mild, have wave induced processes and
231 changes in RSL been of approximately equal importance in the rate of change of the TWL. For
232 beaches with relatively steep foreshores, winter wave height increases have been as much as a

233 factor of six times more important than RSLR during the recent historical period. Allowing
234 beach slopes to vary seasonally (Ruggiero et al., 2005) has little impact on the results presented
235 in Figure 2 (not shown).

236 Performing the same set of analyses as described above for NDBC wave buoy 46002,
237 located seaward of the southern Oregon/northern California coast, reveals that the annual rate
238 of change of wave runup is again positive (~1.8 mm/yr) during the observational record.
239 Therefore while the coastline is emergent relative to processes that affect local mean sea level,
240 this southern stretch of the PNW may in fact be submergent relative to the TWL due to the
241 impact of an increasing wave climate. Figure 3 conceptually illustrates the magnitude and
242 alongshore variability of both RSLR and the time rate of change of wave runup during the
243 historical observational period. While the alongshore resolution of the wave runup
244 computations is poor (only two long-term buoys), it is clear that for at least most of the Oregon
245 coastline, increases in wave runup have made more of a contribution to changes in the TWL
246 than RSLR.

247

248 ***Predicting future changes in TWL***

249

250 To assess the relative impacts of continued wave height increases and SLR on
251 future flood probability and erosion potential along the PNW coast, I first compute how
252 often TWLs impact the backshore (e.g., the toe of a sea cliff) under ‘present’ conditions
253 (Figure 4). The proxy IHPY computed using the 10-year TWL time series described
254 above depends on the foreshore beach slope and on the elevation of the backshore feature
255 of interest. Due to the wave runup dependence on foreshore beach slope, the model
256 predicts higher values of IHPY for steep intermediate to reflective beaches than for

257 shallower sloping dissipative beaches. For a given beach slope, the average number of
258 IHPY decreases with increasing backshore feature elevation (Figure 4). For example, for
259 a representative beach slope of 0.05 our TWL modeling approach suggests that water
260 levels exceeded an elevation of 6 m (relative to ~ Mean Lower Low Water) only about 5
261 hours per year while reaching 4 m over 600 hours per year during the representative
262 decade centered on 2000.

263 Once present conditions are known, both SLR and various projections of
264 continued increases in storminess can be incorporated directly into the representative 10-
265 year TWL time series yielding predictions of the expected future increase in the
266 probability of flooding/erosion events. In Figure 5, the percent increase in IHPY due to
267 RSLR only is computed for a range of possible future conditions. Here the RSLR
268 projections can be thought of either as a range of possible changes by a certain time
269 period, say by 2025 (25 years from year 2000), or simply a magnitude of change not
270 associated with a particular time frame but one that may eventually be reached. Recent
271 projections of multi-decadal SLR (Bindoff et al., 2007, Rahmstorf, 2010) magnitudes of
272 approximately 0.1 m to 0.2 m, assuming the Intergovernmental Panel on Climate
273 Change's (IPCC) A1B Special Report on Emissions Scenarios (SRES) climate scenario
274 and a stationary wave climate, would result in an increase in IHPY of between 20% to
275 140%, depending on the elevation of the backing feature (shown in Figure 5 for a beach
276 slope of 0.05). The IPCC A1B scenario describes a more integrated world characterized
277 by rapid economic growth, technological innovation, increased globalization, and a
278 balance across energy sources so that we are not solely reliant on fossil fuels
279 (Nakicenovic et al., 2000). These curves shift downward for higher sloping beaches and

280 upward for lower sloping beaches where the relative effect of SLR is more important.
281 More extreme estimates of multi-decadal sea level change, up to as much as 0.5 m
282 (Figure 5), could cause an increase in IHPY of as much as 100% to 400%.

283 While uncertain, our ability to predict RSLR is more advanced than our ability to
284 predict future trends in wave climate. Therefore, we first make the simple assumption
285 that the linear rate of increase observed in the wave height record will continue and we
286 restrict our predictions to 25 years from the midpoint of our 10 year time series (2000 to
287 2025). Since the storms responsible for the highest wave runup events occur during the
288 winter it is important to distinguish between the rates of increase of waves as a function
289 of season. Applying the same analysis techniques employed to create Figure 1 (middle
290 panel) to just the winter (summer) wave heights and periods, it is found that their rates of
291 increase are respectively 0.024 m/yr (0.013 m/yr) and 0.0072 s/yr (0.0214 s/yr). As
292 described above, the rate of increase in wave heights is in fact dependent on the
293 exceedance percentile of the SWH CDF. Therefore, the most appropriate method for
294 incorporating predicted increases in wave heights into the 10-year TWL time series is as
295 a function of exceedance percentile. Here we discretize the CDF into 1% probability bins
296 and compute the rate of increase for each bin. Waves that are exceeded only 1% of the
297 time in any given year have increased by a rate of approximately 4.3 cm/yr.

298 Figure 6 illustrates the impact of both a range of RSLR and a continued increase
299 in the intensity of the wave climate on the frequency with which the TWL exceeds
300 various backshore elevations. It is clear that the impact of the combination of RSLR and
301 increasing waves is significantly different than that with RSLR alone (Figure 5). The
302 relative importance of increasing wave heights and periods depends on the magnitude of

303 RSL change, foreshore beach slope, elevation of the backing feature, and the method by
304 which the wave height increases are incorporated into the TWL time series (Figure 7).
305 For RSLR magnitudes of up to 0.15 m by 2025, increasing wave heights contribute more
306 to the increase in IHPY than does SLR. Wave heights become relatively more important
307 with increasing beach slopes and increasing backshore feature elevations. Incorporating
308 the increase in wave heights as a function of exceedance percentile has a more significant
309 impact than simply incorporating seasonal increases or annual increases into the wave
310 height time series (Figure 7).

311 Figure 7 indicates that a RSLR of between 0.15 m and 0.3 m would be more
312 important than wave height increases by approximately 2025. While wave height
313 increases were incorporated using a variety of approaches, in each case the rate of
314 increase was similar to that observed in the recent historical time period. In Figure 8 the
315 RSLR value that will have equal impact on changes to IHPY as increasing wave heights
316 is computed for a variety of changes in the rate of increase in waves. The rate of increase
317 is varied between 20% of and 200% of the observed values.

318

319 ***Discussion***

320 The objective of this paper has been to develop a primary impression of the roles
321 of the various climate controls on coastal hazards, particularly SLR versus increasing
322 wave heights, and to assess their relative importance along the PNW coast with its
323 variability in land-elevation changes. Based on approximately 30 years of recorded waves
324 and tides, and good documentations of the morphologies of PNW beaches, it has been
325 possible to model these relative impacts for any combination of SLR, VLM, or projected

326 increases in storminess and generated waves via assessments of the TWLs from the
327 combined processes. However, this simple approach suffers from two primary
328 limitations. First, the analyses have not accounted for morphological feedbacks, e.g. the
329 toe of the backshore feature is not adjusted to a new equilibrium elevation under
330 changing sea level and erosion by waves. The significance of excluding this negative
331 feedback depends on the resistance of the backshore to erosion. The toe elevation of sea
332 cliffs composed of resistant rock (or shore protection structures) may have a considerable
333 lag in its response to increased impacts while IHPY at the toe of retreating sand dunes
334 may remain approximately constant over the long term in a condition of dynamic
335 equilibrium. Regardless of whether or not these contrasting erosional responses had been
336 included in the analyses, the quantification of the increase in IHPY can be thought of as a
337 proxy for this retreat and therefore still representing an enhancement of coastal
338 vulnerability. A second limitation in the approach is the scientific community's present
339 lack of ability to predict either SLR or the behavior of regional wave climates over the
340 coming decades without significant uncertainty. Here I have taken what is likely a
341 conservative approach by simply extrapolating historical rates into the future. As
342 knowledge of the physics responsible for these climate controls increases, analyses like
343 these can be refined.

344 Changes to the TWL are just one way in which increasing wave heights (and
345 periods) impact coastal hazards. Volumetric sediment transport rates are often
346 formulated as nonlinear functions of wave height (Komar, 1998) and therefore small
347 increases in wave heights can have significant impacts on transport rates, gradients in
348 transport rates, and resulting morphological changes. Slott et al. (2006) found that

349 moderate shifts in storminess patterns and the subsequent effect on wave climates could
350 increase the rate at which shorelines recede or accrete to as much as several times the
351 recent historical rate of shoreline change. On complex-shaped coastlines, including
352 cusped-cape and spit coastlines, they found that the alongshore variation in shoreline
353 retreat rates could be an order of magnitude higher than the baseline retreat rate expected
354 from sea level rise alone over the coming century.

355 Working on a straight, sandy coastline just north of the Columbia River, Ruggiero
356 et al. (2010b) applied a deterministic one-line shoreline change model in a quasi-
357 probabilistic manner to test the effects of both wave climate and sediment supply
358 variability on decadal-scale hindcasts and forecasts. While their modeling exercises
359 indicated that shoreline change is most sensitive to changes in wave direction, the effect
360 of an increasingly intense future wave climate was significant. A wave climatology
361 incorporating increasing winter wave heights and periods resulted in as much as 100 m
362 more erosion than a baseline prediction in which the wave climate remained stationary.
363 As with the TWL modeling, the magnitude of these differences depended on whether the
364 increase in the severity of wave conditions is distributed evenly throughout the entire
365 year or enhanced during the winter storm season. To achieve the same magnitude of
366 additional shoreline change caused by increasing wave heights, approximately 100 m, a
367 simple Bruun Rule calculation (Bruun, 1962) indicates that sea level would have to rise
368 over 0.5 m by approximately 2025.

369

370 **Conclusions**

371 The primary outcome of this work is a direct assessment of the relative
372 contributions of various climate controls on coastal exposure to high water levels. Over

373 the historical period of observations (since the early-1980s) the buoy-measured increases
374 in deep-water wave heights and periods have been more responsible for increasing the
375 frequency of coastal erosion and flooding events along the PNW coast than changes in
376 sea level. While this is true for stretches of the PNW coast in which RSL change is
377 approximately the same as global SLR (north-central Oregon coast), trends in wave
378 induced processes have been potentially more important along the southern Oregon coast
379 where VLMs are significant. Under a range of future multi-decadal climate change
380 scenarios, increasing storm wave heights may continue to increase the probability of
381 coastal flooding/erosion more than SLR induced changes alone. The combination of each
382 of these climate controls on the TWL occurring simultaneously could cause as much as a
383 factor of five increase in erosion/flood frequency over the coming decades.

384

385 **Acknowledgements**

386 The author gratefully acknowledges the support of NOAA's Sectoral Applications
387 Research Program (SARP) under NOAA Grant# NA08OAR4310693 and NOAA's
388 National Sea Grant College Program under NOAA Grant's #NA06OAR4170010.

389

390 **References**

391 Allan, J.C. and Komar, P.D., 2000. Are ocean wave heights increasing in the eastern
392 North Pacific? *EOS, Trans. AGU*, 47, 561-567.

393 Allan, J. C. and P. D. Komar. 2002. Extreme storms on the Pacific Northwest Coast
394 during the 1997-98 El Niño and 1998-99 La Niña. *Journal of Coastal Research*,
395 18, 175-193.

396 Allan, J. C., and P.D. Komar, 2006. Climate controls on US West Coast erosion
397 processes: *J. Coastal Res.*, 22, 511-529.

398 Allan, J.C., Ruggiero, P., and Roberts, J., 2010. Coastal Flood Insurance Study, Coos
399 County, Oregon, Oregon Department of Geology and Mineral Industries Report to
400 the Federal Emergency Management Agency, Portland, Oregon, 131 pp.

401 Bacon, S. and Carter, D. J. T., 1991. Wave climate changes in the North Atlantic and
402 North Sea, *Int. J. of Climatol.*, 11, 545-558.

403 Bindoff, N.L., J. Willebrand, V. Artale, A. Cazenave, J. Gregory, S. Gulev, K. Hanawa,
404 Le Quéré, S. Levitus, Y. Nojiri, C.K. Shum, L.D. Talley, and A. Unnikrishnan,
405 2007. Observations: oceanic climate change and sea level. In: *Climate Change*
406 *2007: The Physical Science Basis*. Contribution of Working Group I to the Fourth
407 Assessment Report of the Intergovernmental Panel on Climate [Solomon, S., D.
408 Qin, M. Manning, Z. Chen, M. Marquis, K.B. Avery, M. Tignor, and H.L. Miller
409 (eds.)]. Cambridge University Press, Cambridge, UK and New York, pp. 385-432.

410 Bruun, P. 1962. Sea-level rise as a cause of shore erosion. *Journal of Waterways Harbors*
411 *Division*, American Society of Civil Engineers, 88, 117-130.

412 Burgette, R.J., Weldon, R.J II, and Schmidt, D.A, 2009. Interseismic uplift rates for
413 western Oregon and along-strike variation in locking on the Cascadia subduction
414 zone, *J. Geophys. Res.*, 114, B01408, doi:10.1029/2008JB005679.

415 Carter, D., and L. Draper, 1988. Has the north-east Atlantic become rougher?, *Nature*.

416 Church, J. A., and N. J. White, 2006. A 20th century acceleration in global sea-level rise,
417 *Geophys. Res. Lett.*, 33, L01602, doi:10.1029/2005GL024826.

418 Collins, B. and Sitar, N., 2008. Processes of coastal bluff erosion in weakly lithified

419 sands, Pacifica, California, USA, *Geomorphology*, 97, 483-501.

420 Enfield, D.B., and Allan, J.S., 1980. On the structure and dynamics of monthly mean sea
421 level anomalies along the Pacific coast of North and South America, *J. Phys.*
422 *Oceanogr.*, 10, 557-578.

423 Favre, A., and A. Gershunov. 2006. Extra-tropical cyclonic/anticyclonic activity in
424 North-Eastern Pacific and air temperature extremes in Western North America.
425 *Climate Dynamics*, 26, 617–629.

426 Flick, R.E., Murray, J.F., and Ewing, L.C., 2003. Trends in United States Tidal Datum
427 Statistics and Tide Range. *J. Waterway, Port, Coastal, Ocean Eng.* 129, 155,
428 doi:10.1061/(ASCE)0733-950X(2003)129:4.

429 Gemmrich, J., Thomas, B., and Bouchard, R., 2011. Observational changes and trends in
430 northeast Pacific wave records, *Geophysical Research Letters*, 38, L22601,
431 doi:10.1029/2011GL049518.

432 Geng, Q., and Sugi, M. 2003. Possible change of extratropical cyclone activity due to
433 enhanced greenhouse gases and sulfate aerosols: Study with a high-resolution
434 AGCM, *J. Clim.*, 16, 2262–2274.

435 Graham, N.E., and H.F. Diaz, 2001. Evidence for intensification of North Pacific winter
436 cyclones since 1948: *Bulletin of the American Meteorological Society*, 82, 1869-
437 1893.

438 Hapke, C. and Plant, N, 2010. Predicting coastal cliff erosion using a Bayesian
439 probabilistic model, *Marine Geology*, 278, 140-149,
440 doi:10.1016/j.margeo.2010.10.001.

441 Harris, E.L., 2011. Assessing physical vulnerability of the coast in light of a changing

442 climate: An integrated, multi-hazard, multi-timescale approach, unpublished MS
443 thesis, Oregon State University, Corvallis, OR, 77 pp.

444 Holman, R.A., 1986. Extreme value statistics for wave run-up on a natural beach, *Coast.*
445 *Eng.*, 9, 527-544.

446 Kaminsky, G., Ruggiero, P. and Gelfenbaum, G., 1998. Monitoring coastal change in
447 Southwest Washington and Northwest Oregon during the 1997/98 El Niño, *Shore*
448 *and Beach*, 66 (3), 42-51.

449 Knutson, T. R., J. L. McBride, J. Chan, K. Emanuel, G. Holland, C. Landsea, I. Held, J.
450 P. Kossin, A. K. Srivastava, and M. Sugi (2010), Tropical cyclones and climate
451 change, *Nature Geoscience*, 3(3), 157–163, doi:10.1038/ngeo779.

452 Komar, P. D. 1998. The 1997-98 El Niño and erosion of the Oregon coast. *Shore &*
453 *Beach*, 66, 33-41.

454 Komar, P.D., 1998. Beach processes and sedimentation, Second edition, Prentice Hall,
455 Saddle River, N.J., 544 pp.

456 Komar, P.D., Allan, J.C., and Ruggiero, P., 2011. Sea level variations along the US
457 Pacific Northwest coast: tectonic and climate controls, *Journal of Coastal*
458 *Research*, (27) 5, 808-823, DOI:10.2112/JCOASTRES-D-10-00116.1.

459 McCabe, G. J., M. P. Clark, and M. C. Serreze. 2001. Trends in northern hemisphere
460 surface cyclone frequency and intensity. *Journal of Climate*, 14, 2763–2768.

461 Méndez, F.J., Menéndez, M., A. Luceno, and I. J. Losada, 2006. Estimation of the long-
462 term variability of extreme significant wave height using a time-dependent Peak
463 Over Threshold (POT) model, *J. Geophys. Res.*, 111, C07024,

464 doi:10.1029/2005JC003344.

465 Mendez, F. J., M. Menendez, A. Luceno, and I. J. Losada, 2006. Estimation of the long-
466 term variability of extreme significant wave height using a time-dependent Peak Over
467 Threshold (POT) model, *J. Geophys. Res.*, 111, C07024, doi:10.1029/2005JC003344.

468 Menéndez, M., Méndez, F.J., Losada, I. J., and Graham, N.E., 2008. Variability of
469 extreme wave heights in the northeast Pacific Ocean based on buoy
470 measurements, *Geophys. Res. Lett.*, 35(22), doi:10.1029/2008GL035394.

471 Nakicenovic, N., J. Alcamo, G. Davis, B. de Vries, J. Fenhann, S. Gaffin, K. Gregory, A.
472 Grubler, T.Y. Jung, T. Kram, E.L. La Rovere, L. Michaelis, S. Mori, T. Morita,
473 W. Pepper, H. Pitcher, L. Price, K. Riahi, A. Roehrl, H.H. Rogner, A. Sankovski,
474 M. Schlesinger, P. Shukla, S. Smith, R. Swart, S. van Rooijen, N. Victor, and Z.
475 Dadi, 2000. Special Report on Emissions Scenarios: A Special Report of Working
476 Group III of the Intergovernmental Panel on Climate Change, N. Nakicenovic and
477 R. Swart (eds). Cambridge University Press, Cambridge, United Kingdom, 570
478 pp.

479 National Data Buoy Center (NDBC), 2008. National Data Buoy Center, National
480 Oceanographic and Atmospheric Administration. <http://seaboard.ndbc.noaa.gov/>
481 (accessed April 1, 2008).

482 Nichols, R.J. and Tol, R.S.J., 2006. Impacts and responses to sea-level rise: a global
483 analysis of the SRES scenarios over the twenty-first century, *Phil. Trans. R. Soc.*
484 *A*, doi: 10.1098/rsta.2006.1754, 364 (1841), 1073-1095.

485 National Ocean Service (NOS), 2009. NOAA Tides and Currents: Center for Operational
486 Oceanographic Products and Services. <http://www.co-ops.nos.noaa.gov/> (accessed

487 April 1, 2010).

488 Rahmstorf, S., 2007. A Semi-Empirical Approach to Projecting Future Sea-Level Rise
489 *Science*, 315 (5810), DOI: 10.1126/science.1135456.

490 Rahmstorf, S. 2010. A new view on sea level rise. *Nature*, 4, 44-45.

491 Ruggiero, P., Komar, P.D., McDougal, W.G. and Beach, R.A., 1996. Extreme water
492 levels, wave runup, and coastal erosion, *Proceedings 25th Coastal Engineering*
493 *Conference, ASCE*, 2793-2805.

494 Ruggiero, P., Komar, P.D., McDougal, W.G., Marra, J.J., and Beach, R.A., 2001. Wave
495 runup, extreme water levels and the erosion of properties backing beaches, *J.*
496 *Coastal Res.*, 17(2), 407-419.

497 Ruggiero, P., Holman, R.A., and Beach, R.A., 2004. Wave runup on a high-energy
498 dissipative beach, *Journal of Geophysical Research*, Vol. 109, C06025,
499 doi:10.1029/2003JC002160, 2004.

500 Ruggiero, P., Kaminsky, G.M., Gelfenbaum, G., and Voigt, B., 2005. Seasonal to
501 interannual morphodynamics along a high-energy dissipative littoral cell, *Journal*
502 *of Coastal Research*, 21(3), 553-578.

503 Ruggiero, P., Komar, P.D., Allan, J.C., 2010a. Increasing wave heights and extreme-
504 value projections: the wave climate of the U.S. Pacific Northwest, *Coastal*
505 *Engineering*, 57, 539-552, doi:10.1016/j.coastaleng.2009.12.005.

506 Ruggiero, P., Buijsman, M.C., Kaminsky, G., and Gelfenbaum, G., 2010b. Modeling the
507 effect of wave climate and sediment supply variability on large-scale shoreline
508 change, *Marine Geology*, 273, 127-140, DOI:10.1016/j.margeo.2010.02.008.

509 Sallenger, A. H. 2000. Storm impact scale for barrier islands. *Journal of Coastal Research*
510 16:890-895.

511 Seymour, R.J., 2011. Evidence for Changes to the Northeast Pacific Wave Climate
512 *Journal of Coastal Research*, 27(1), 194-201, DOI: 10.2112/JCOASTRES-D-09-
513 00149.1

514 Slott, J.M., Murray, A.B., Ashton, A.D., Crowley, T.J., 2006. Coastline responses to
515 changing storm patterns, *Geophys. Res. Lett.*, 33, 33(L18404):
516 DOI10.1029/2006GL027445.

517 Stockdon, H.F., R.A. Holman, P.A. Howd, and A.H. Sallenger, 2006. Empirical
518 parameterization of setup, swash, and runup, *Coast. Eng.*, 53(7), pp. 573-588.

519 Stockdon, H.F., Sallenger, A.H., Holman, R.A., and Howd, P.A., 2007. A simple model
520 for the spatially-variable coastal response to hurricanes, *Mar. Geol.*, 238, 1-20.

521 Wang, X.L., Zwiers, F.W., and Swail, V.R. (2004). “ North Atlantic ocean wave climate
522 change scenarios for the twenty-first century”. *J. Climate*, 17, 2368-2383.

523 Wang, X.L. and Swail, V.R. (2006). “ Climate change signal and uncertainty in
524 projections of ocean wave heights”. *Climate Dyn.*, 26, 109-126.

525 Yin, J. H. 2005. A consistent poleward shift of the storm tracks in simulations of 21st
526 century climate, *Geophysical Research Letters*, 32, L18701.

527 Young, I.R., Zieger, S., and Babanin, A.V., 2011. Global trends in wind speed and wave
528 height, *Science* 332, 451, DOI: 10.1126/science.1197.

Figure1

[Click here to download high resolution image](#)

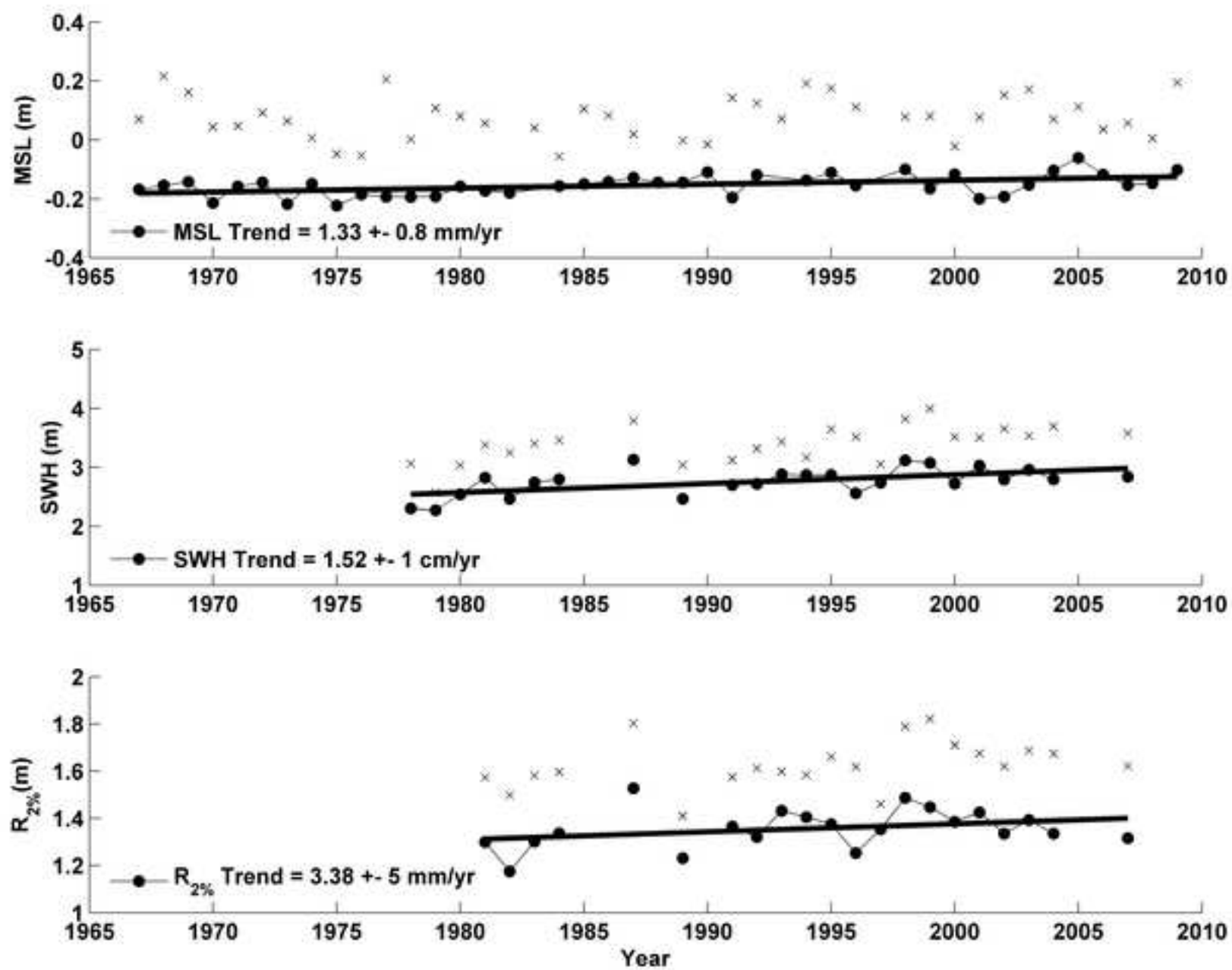


Figure2
[Click here to download high resolution image](#)

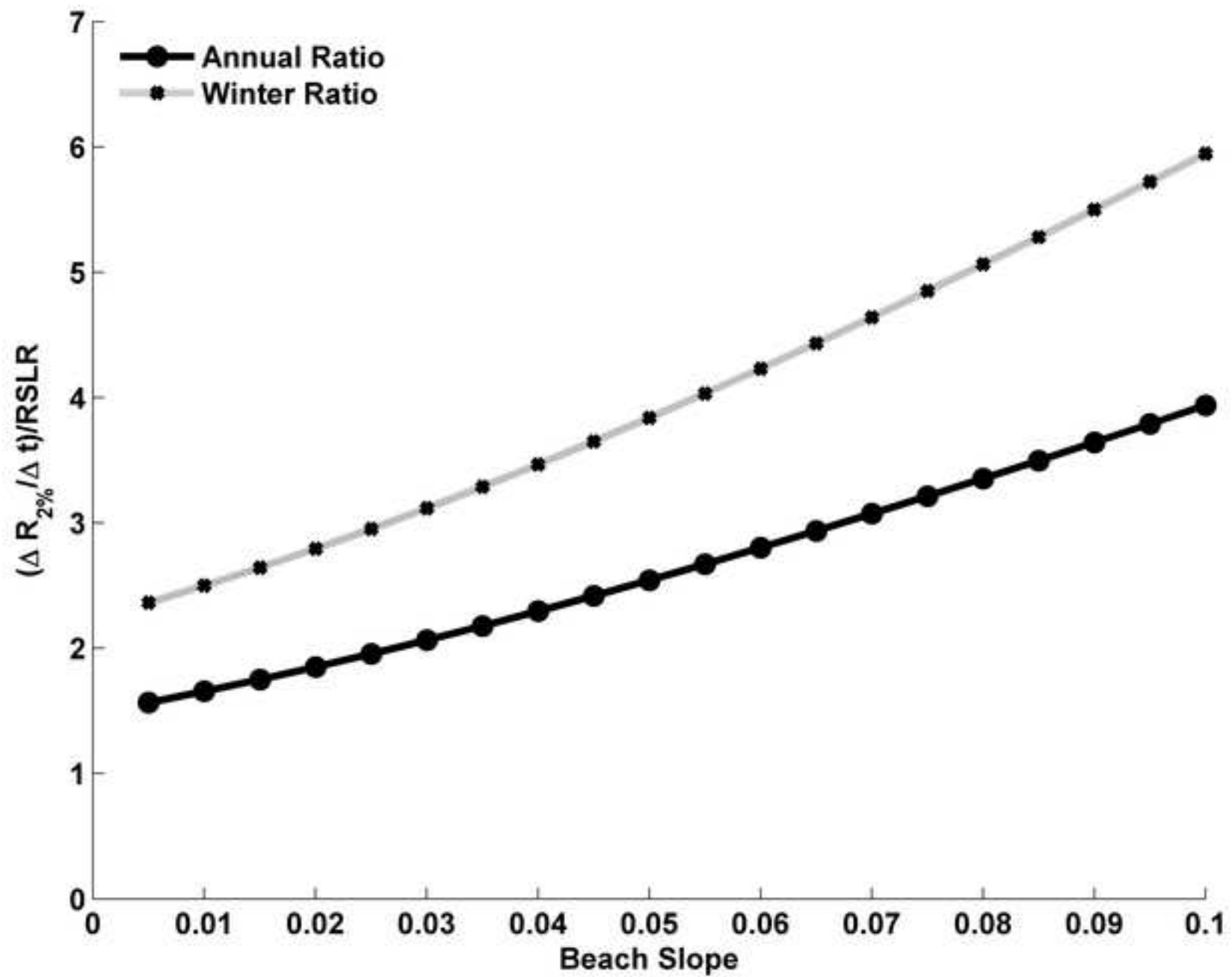


Figure3
[Click here to download high resolution image](#)

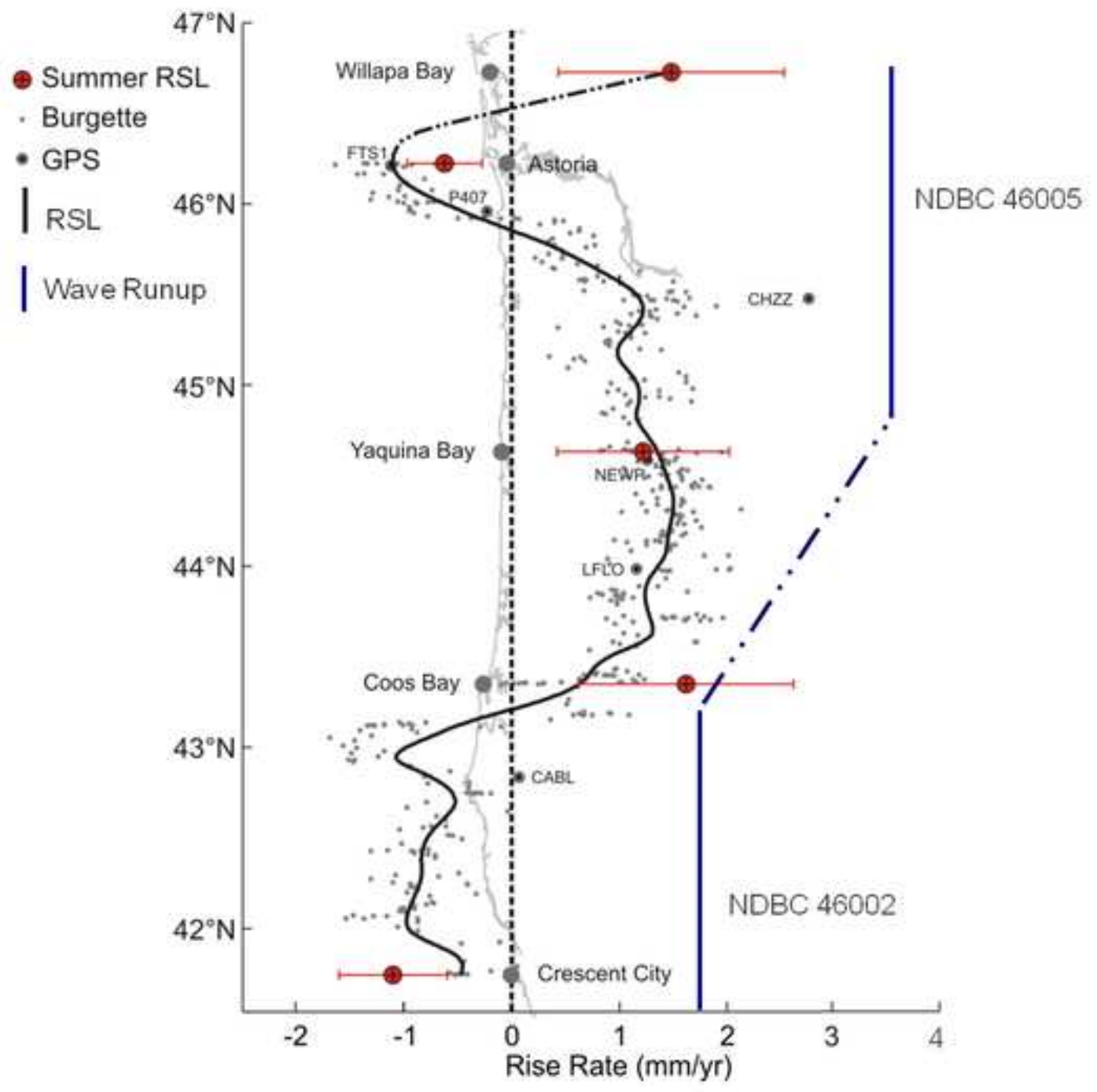


Figure4
[Click here to download high resolution image](#)

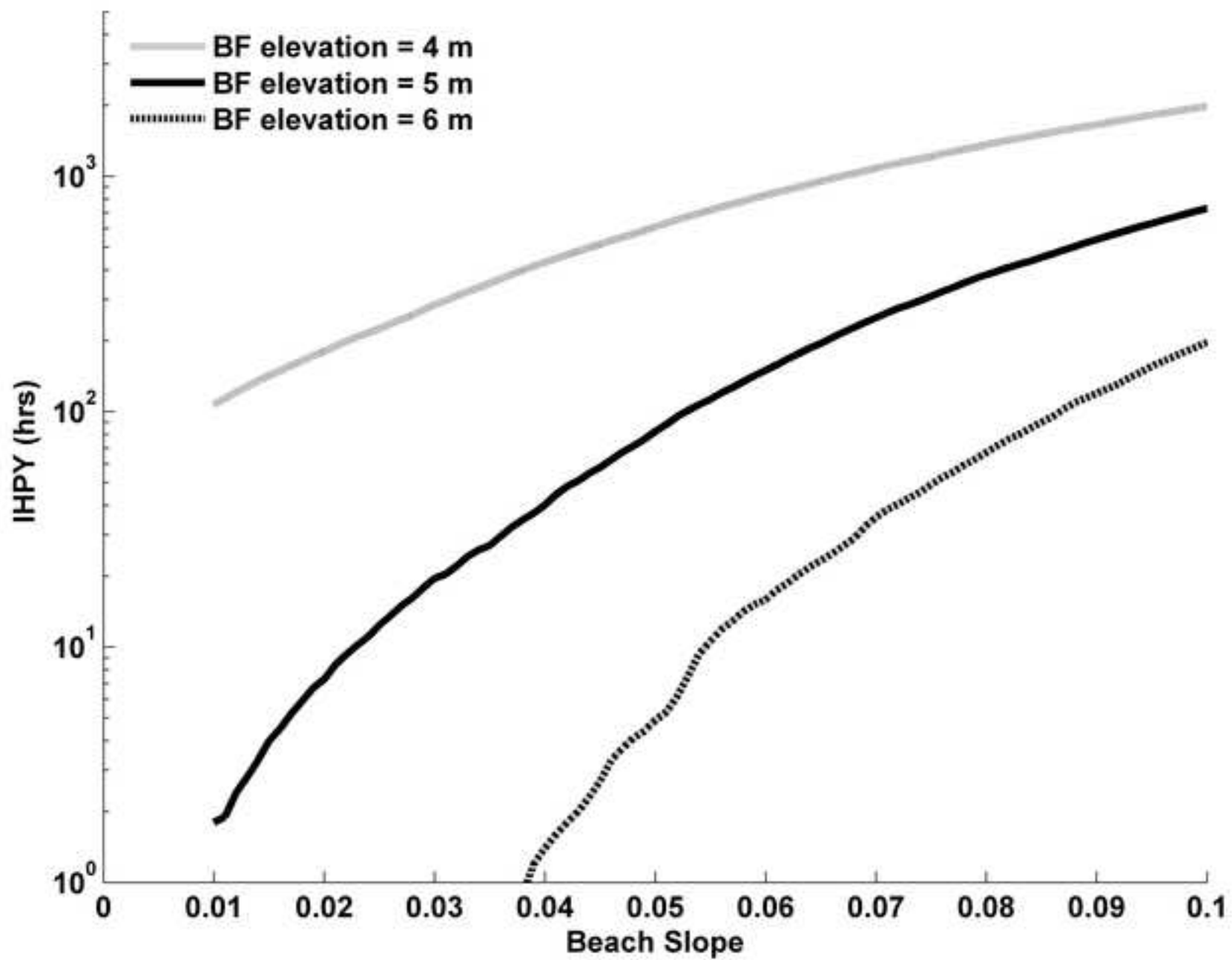


Figure5
[Click here to download high resolution image](#)

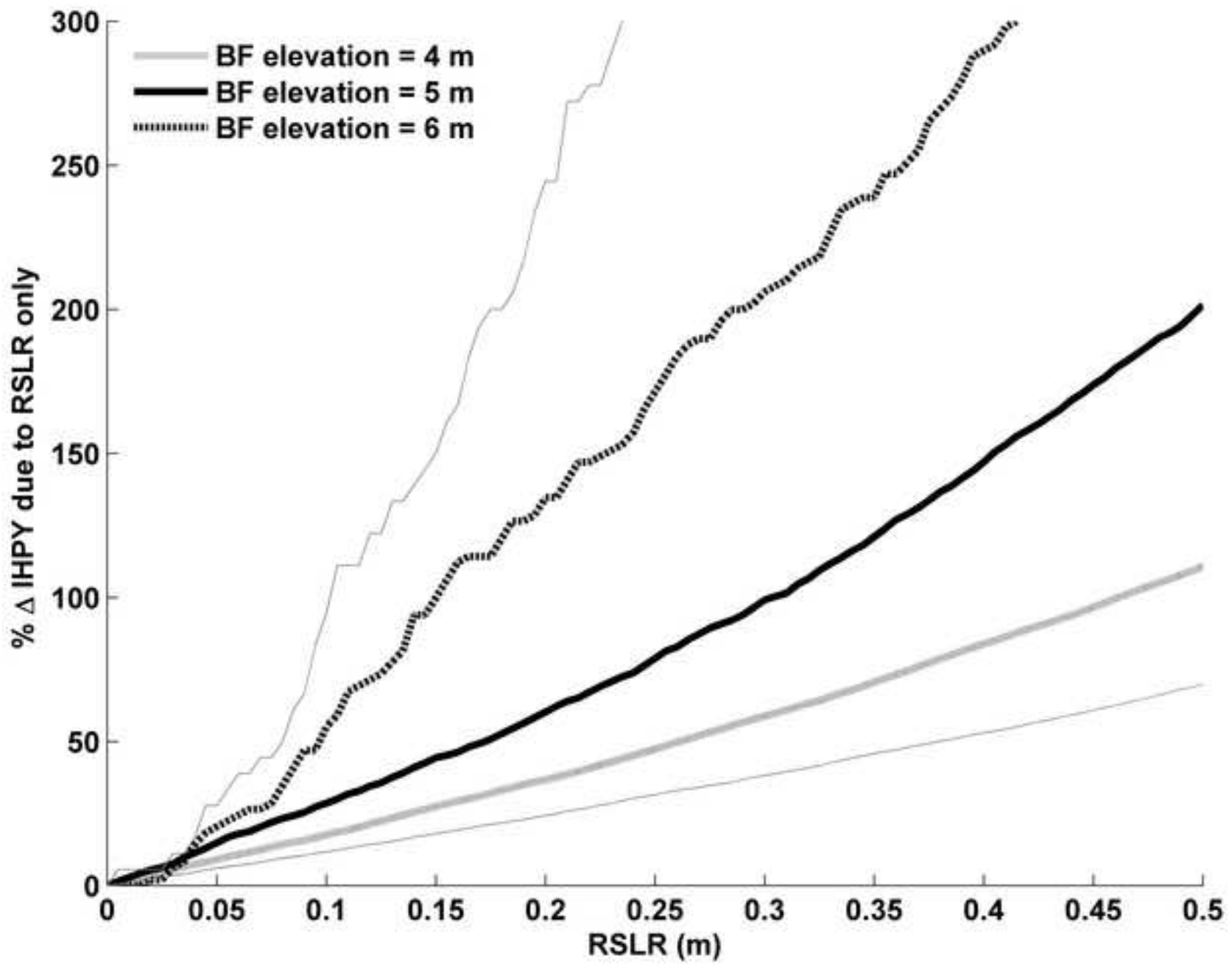


Figure6
[Click here to download high resolution image](#)

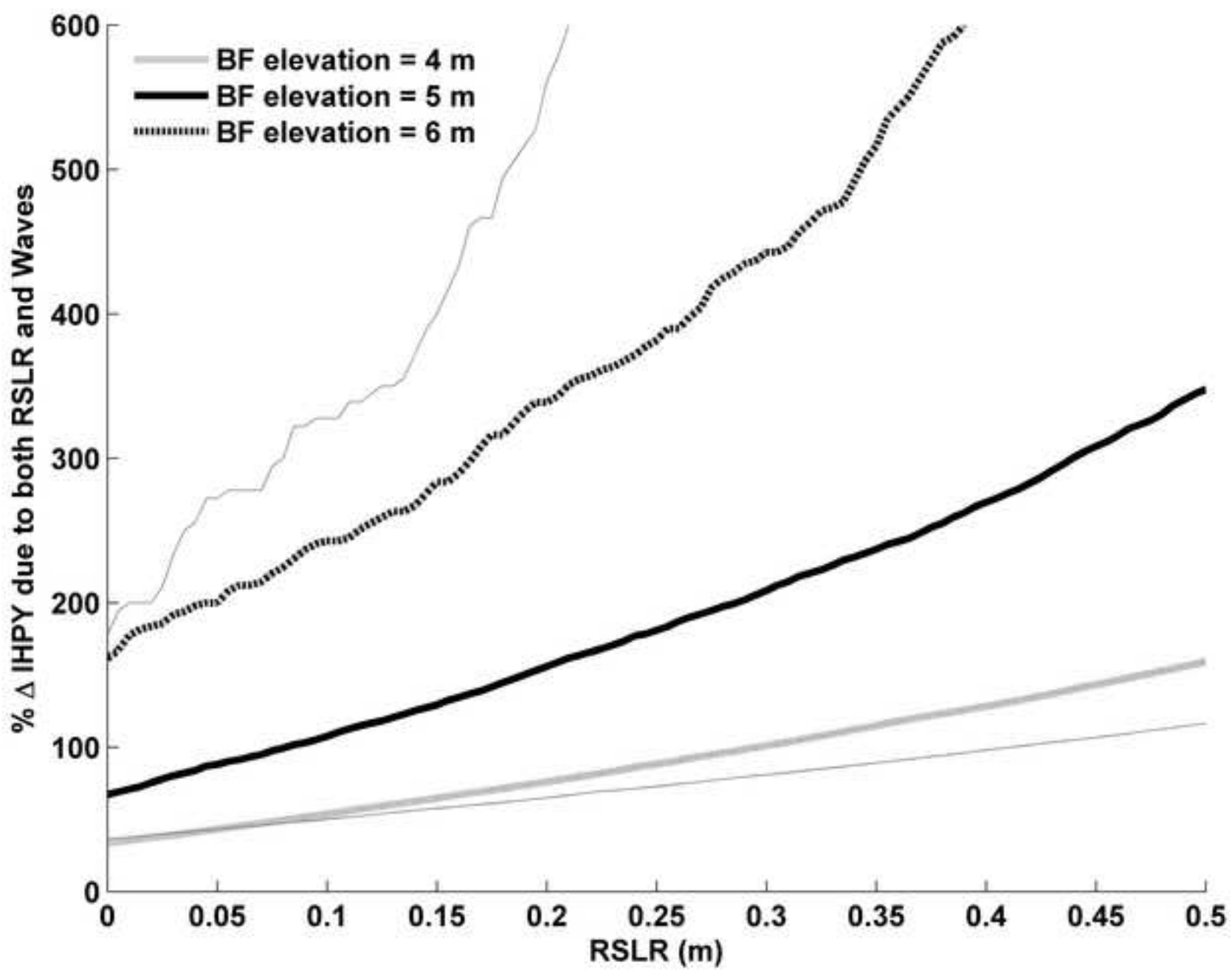


Figure 7
[Click here to download high resolution image](#)

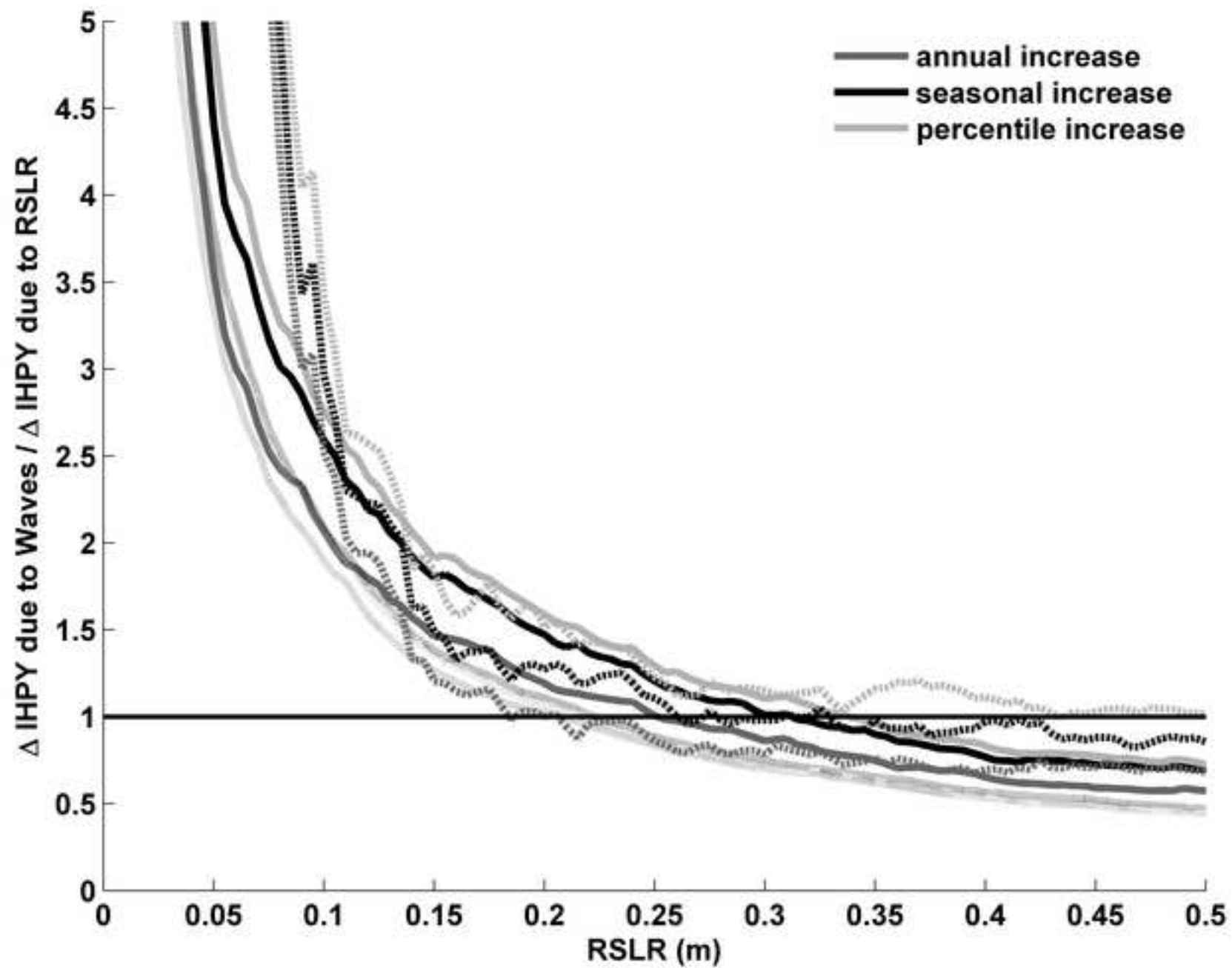
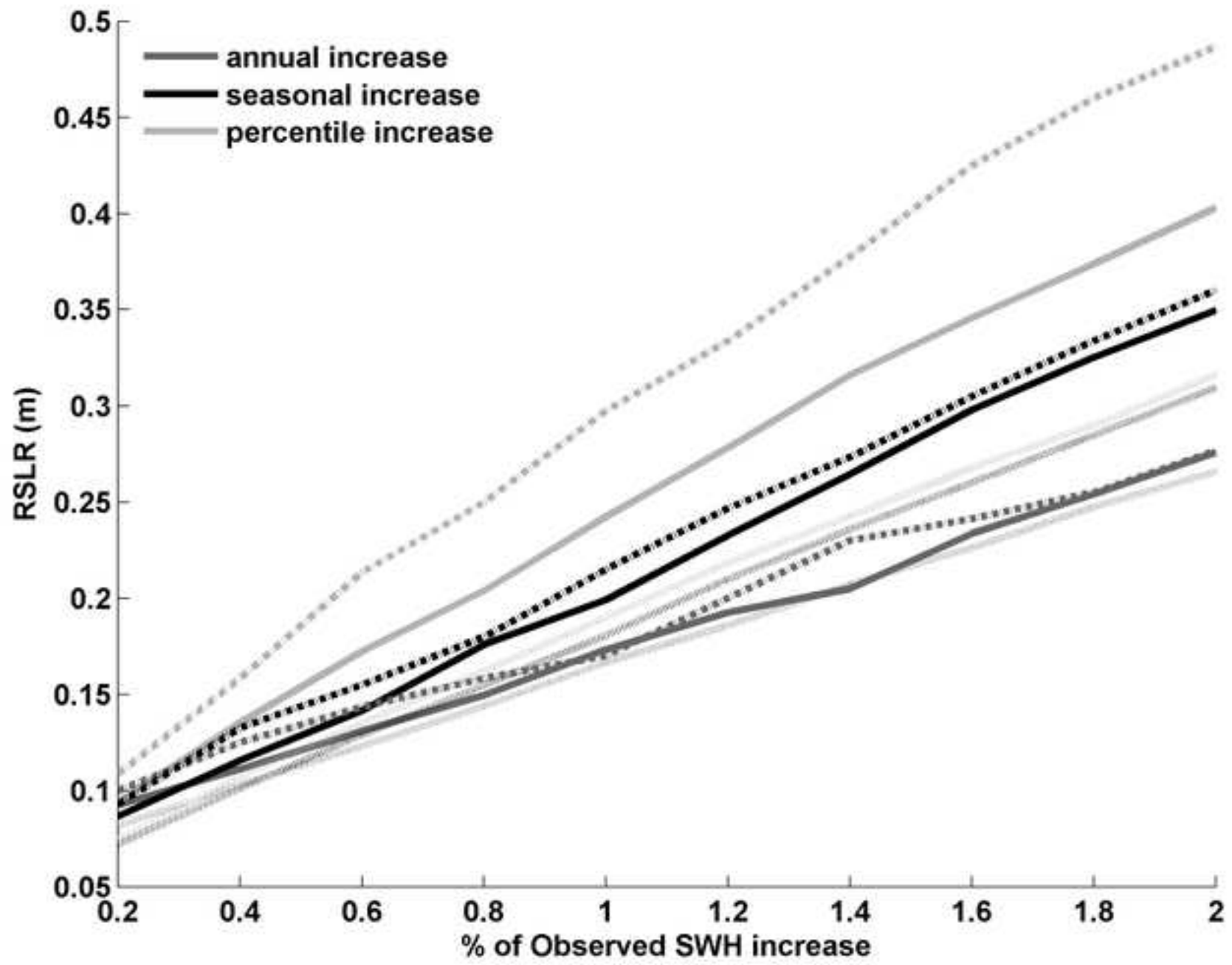


Figure8
[Click here to download high resolution image](#)



1 **Figure Captions**

2 Figure 1. top panel) Trends and variations in summer average (solid line) and winter
3 average (symbols only) RSLs for the Yaquina Bay tide-gauge record. Middle panel)
4 Trends and variations in annual average significant wave heights (solid line) and winter
5 average wave heights (symbols only) from NDBC buoy 46005. Bottom panel) Trends
6 and variations in annual average (solid line) and winter average (symbols only) two
7 percent exceedance wave runup values computed using equation 2 and a representative
8 foreshore beach slope of 0.05.

9

10 Figure 2. Ratio of the annual average time rate of change in wave runup (computed using
11 NDBC 46005 wave data and Equation 2) versus RSLR (from the Yaquina Bay tide gage)
12 as a function of average foreshore beach slope. The dashed line is the ratio of winter
13 average runup change rate versus RSLR.

14

15 Figure 3. Alongshore variability of rate of change of wave runup (computed using wave
16 data from NDBC buoys 46005 and 46002, Equation 2, and a foreshore beach slope of
17 0.05) versus RSLR for the Oregon coast (blue lines). Assessments of changes in RSLs are
18 based on tide-gauge records compared with benchmark and GPS measurements of land-
19 elevation changes (after Burgette et al., 2009), with their corresponding RSL rates
20 obtained by adding 2.28 mm/y as an estimate of the regional PNW rise in sea level.
21 (modified from Komar et al., 2011)

22

23 Figure 4. Impact hours per year (IHPY) of the TWL for a range of foreshore beach slopes
24 and three backshore feature (BF) elevations (e.g., sea cliff toe or dune crest elevation).

25

26 Figure 5. Percent increase in IHPY due to SLR only, relative to approximately year 2000,
27 for a range of RSLR magnitudes and three backshore feature (BF) elevations. Thick lines
28 show computations for a beach slope of 0.05 while the thin black lines show the influence
29 of various beach slopes for BF=5 m (higher line for slope = 0.01 and lower line for slope
30 = 0.1).

31

32 Figure 6. Percent increase in IHPY due to both SLR and wave height increases, relative
33 to approximately year 2000, for a range of RSLR magnitudes and three backshore feature
34 (BF) elevations. Thick lines show computations for a beach slope of 0.05 while the thin
35 black lines show the influence of various beach slopes for BF=5 m (higher line for slope
36 = 0.01 and lower line for slope = 0.1).

37

38 Figure 7. Ratio of the increase in IHPY due to wave height changes only to IHPY
39 increases due to SLR only for a range of SLR scenarios by approximately 2025 (relative
40 to 2000) and 3 backshore feature elevations (line types same as Figure 6). The dark grey
41 lines represent annual increases in wave heights incorporated into the TWL, while the
42 black lines represent inclusion of seasonal trends and the light grey lines represent rates
43 of increase of various percentiles respectively.

44

45 Figure 8. The RSLR magnitude that would have the same impact on IHPY as wave
46 height increases for a range of possible future wave climates. The wave climate is
47 allowed to vary between 20% and 200% of observed recent historical rates. Line symbols
48 and colors represent the same combinations of BF elevations and approach for inclusion
49 of wave height increases into the TWL as in Figures 6 and 7.